Inorganic Chemistry

ARTICLE

pubs.acs.org/IC

The Rich Chemistry of $[Zn_2Cp^*_2]$: Trapping Three Different Types of Zinc Ligands in the $PdZn_7$ Complex $[Pd(ZnCp^*)_4(ZnMe)_2\{Zn(tmeda)\}]$

Timo Bollermann,[†] Kerstin Freitag,[†] Christian Gemel,[†] Mariusz Molon,[†] Rüdiger W. Seidel,[‡] Moritz von Hopffgarten,[§] Paul Jerabek,[§] Gernot Frenking,[§,*] and Roland A. Fischer[†,*]

[†]Anorganische Chemie II - Organometallics & Materials, Ruhr-Universität Bochum, D-44780 Bochum,Germany

[‡]Lehrstuhl für Analytische Chemie, Ruhr-Universität Bochum, D-44780 Bochum, Germany

[§]Department of Chemistry, Philipps University Marburg, D-35032 Marburg, Germany

Supporting Information

ABSTRACT: The synthesis, structural characterization, and bonding situation analysis of a novel, *all*-zinc, hepta-coordinated palladium complex $[Pd(ZnCp^*)_4(ZnMe)_2\{Zn(tmeda)\}]$ (**1**) is reported. The reaction of the substitution labile d^{10} metal starting complex $[Pd(CH_3)_2(tmeda)]$ (tmeda = *N*,*N*,*N*′,*N*′-tetramethyl-ethane-1,2-diamine) with stoichiometric amounts of $[Zn_2Cp^*_2]$ (Cp^* = pentamethylcyclopentadienyl) results in the formation of $[Pd(ZnCp^*)_4(ZnMe)_2\{Zn(tmeda)\}]$ (**1**) in 35% yield. Compound **1** has been fully characterized by single-crystal X-ray diffraction, ^1H and ^{13}C NMR spectroscopy, IR spectroscopy, and liquid injection field desorption ionization mass spectrometry. It consists of an unusual $[PdZn_7]$ metal core and exhibits a terminal $\{Zn(tmeda)\}$ unit. The bonding situation of **1** with respect to the properties of the three different types of Zn ligands Zn(R,L) (R = CH_3, Cp^*; L = tmeda) bonded to the Pd center was studied by density functional theory quantum chemical calculations. The results of energy decomposition and atoms in molecules analysis clearly point out significant differences according to R vs L. While $Zn(CH_3)$ and $ZnCp^*$ can be viewed as 1e donor Zn(I) ligands, $\{Zn(tmeda)\}$ is best described as a strong 2e Zn(0) donor ligand. Thus, the 18 valence electron complex **1** nicely fits to the family of metal-rich molecules of the general formula $[M(ZnR)_a(GaR)_b]$ ($a + 2b = n \geq 8$; M = Mo, Ru, Rh; Ni, Pd, Pt; R = Me, Et, Cp^*).

INTRODUCTION

The discovery of $[Zn_2Cp^*_2]$ (Cp^* = pentamethylcyclopentadienyl) with an unsupported covalent Zn(I)−Zn(I) bond by Carmona et al. in 2004 stimulated much research on related compounds with a core unit $[Zn_2]^{2+}$.[1−3] Initially, the focus was on the detailed descriptions of the electronic structure including characteristics of the bonding situation and related spectroscopic data, i.e., IR and Raman spectroscopy.[4−7] Later on, the chemistry of $[Zn_2Cp^*_2]$ was investigated, in particular with respect of Lewis acid/base adducts and the substitution of the Cp^* ligand without cleavage of the Zn−Zn bond.[8−13] However, the chemistry of $[Zn_2Cp^*_2]$ with highly reactive transition metal complexes $[ML_n]$ remained unexplored. Recently, we found that $[Zn_2Cp^*_2]$ behaves as a convenient source for the one-electron ligands $ZnCp^*$ and $\{ZnZnCp^*\}$, which is of importance within the scope of our work on 18-electron, Zn-rich complexes of the general formulas $[M(ZnR)_n]$ and $[M(ZnR)_a(GaR)_b]$ ($a + 2b = n \geq 8$; M = Mo, Ru, Rh; Ni, Pd, Pt; R = Me, Et, Cp^*).[14,15] For instance, the reaction of *all*-gallium coordinated d^{10} metal complexes $[M(GaCp^*)_4]$ (M = Pd, Pt) with $[Zn_2Cp^*_2]$ yields the Ga/Zn mixed hexa-coordinated $[M(GaCp^*)_2(ZnCp^*)_2(ZnZnCp^*)_2]$ and the *all*-zinc octa-coordinated $[M(ZnCp^*)_4(ZnZnCp^*)_4]$.[16] The mechanism, as characterized by in situ NMR studies, involves the trapping of $ZnCp^*$ fragments at (unsaturated) intermediates of the type $[L_aM(ZnCp^*)_b]$ (L = $GaCp^*$ or $ZnCp^*$) as well as Cp^* transfer between coordinated $ZnCp^*$ ligands and free $[Zn_2Cp^*_2]$ resulting in release of $ZnCp^*_2$ and binding of $\{ZnZnCp^*\}$ to the transition metal. Accordingly, we started to study the reactivity of $[Zn_2Cp^*_2]$ toward transition metal complexes without the $GaCp^*$ ligands in the coordination sphere. With the olefin complexes $[M(cod)_2]$ (M = Ni, Pt) as reaction partners an interesting combination of Cp^* transfer, release of elemental Zn and trapping of $ZnCp^*$ to yield the products $[Cp^*M(ZnCp^*)_3]$ was found.[17]

These observations prompted us to further explore the reactivity of $[Zn_2Cp^*_2]$ against other substitution labile transition metal complexes. The d^{10} metal complex $[Pd(CH_3)_2(tmeda)]$ (tmeda = *N*,*N*,*N*′,*N*′-tetramethyl-ethane-1,2-diamine) was selected, because we previously found it particularly useful for preparation of metal-rich compounds such as $[Pd_3(InCp^*)_8]$.[18] Herein, Pd(II) is reduced to Pd(0) by quantitative methyl-group transfer to In(I) releasing the In(III) species $[(CH_3)_2InCp^*]$ and free tmeda. With $[Zn_2Cp^*_2]$ instead of $InCp^*$ a similar methyl-transfer to zinc may be anticipated, but the tmeda ligand may not innocent, as Lewis bases L are known to form asymmetric adducts of the general type $[Cp^*L_2ZnZnCp^*]$ as previously reported by Carmona et al. and Schulz et al.[9,10,12] In fact, we obtained and isolated the most unusual title compound $[Pd(ZnCp^*)_4(ZnMe)_2\{Zn(tmeda)\}]$ (**1**). The formation, structural characterization and detailed analysis of the bonding situation of **1** in connection with the above cited series of Zn-rich compounds $[M(ZnR)_n]$ is reported.

Received: August 5, 2011
Published: September 19, 2011

Scheme 1. Synthesis of Compound 1

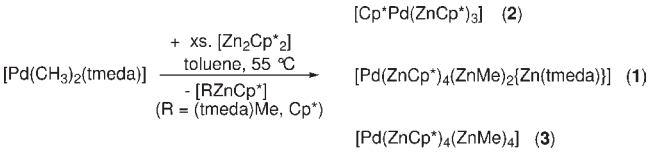

RESULTS AND DISCUSSION

Synthesis, Analytical, and Structural Characterization. Treatment of $[Pd(CH_3)_2(tmeda)]$ with four equivalents of $[Zn_2Cp^*_2]$ in toluene at 55 °C leads to an immediate color change of the homogeneous solution to deep red, and the compound $[Pd(ZnCp^*)_4(ZnMe)_2\{Zn(tmeda)\}]$ (**1**) was collected as yellow crystals (34% yield, based on Pd) after standard workup and purification procedures (Scheme 1 and Experimental Section).

Major amounts of $[ZnCp^*_2]$ and $[Cp^*Pd(ZnCp^*)_3]$[17] (**2**, 33% yield, based on Pd) as well as $[Pd(ZnCp^*)_4(ZnMe)_4]$[15] (**3**, < 5% yield, based on Pd) were isolated as byproduct. Deposition of elemental zinc or palladium, free tmeda, and evolution of ethane were not observed. ^{1}H NMR (in situ) and liquid injection field desorption ionization mass spectrometry (LIFDI-MS) (ex situ) studies reveal a 1:1 molar ratio (±0.1) of the two main products **1** and **2** (>95%) and only traces of **3** (<5%) in the reaction solution. However, the yields of the isolated crystalline products depend on the workup procedure which is mainly based on fractional extraction and subsequent crystallization and the success depends much on the amount of solvent used in the actual procedure (see Experimental Section). The formation pathways of the compounds **1**, **2**, and **3** are likely to be interconnected with each other, competing, and obviously involve homolytic cleavage processes such as Zn−Cp* and Zn−Zn bond cleavage of the starting material $[Zn_2Cp^*_2]$ as it was found in case of $[Pd(ZnCp^*)_4(ZnZnCp^*)_4]$.[16,19−21] In addition, exchange processes involving the organic groups R, i.e., Cp*/CH_3, between Zn and Pd centers has to be taken into account which in turn leads to release of the Zn(II) species $ZnCp^*_2$ and some $[(tmeda)(CH_3)ZnCp^*]$ and the trapping of $\{Zn(tmeda)\}$ and ZnR (R = Me, Cp*) ligands at the Pd centers of **1** and **2**, respectively. Finally, some Zn-bridged Pd species may play a role as intermediates as well. These intermediate species allow transfer of ZnR groups (R = Me, Cp*) between Pd centers, which could be relevant for formation of **3**. Known examples for bridging ZnR units are $[(CpNi)_2(ZnCp)_4]$[22] and $[Pd_2Zn_6Ga_2(Cp^*)_5(CH_3)_3]$.[23] In any case, a rigorous experimental elucidation of the mechanistic details of the formation of **1**−**3** poses a great challenge due to several competing reaction schemes and requires more sophisticated spectroscopic techniques which is beyond the scope of this work. Note, the characterization of the Cp* transfer product **2** has been reported in detail together with the Ni and Pt congeners.[17] Additionally, compound **3** was independently obtained in good yields by reacting $[Pd(GaCp^*)_4]$ with excess $ZnMe_2$ as reported by our group in the recent past.[15] Herein, we now present a detailed discussion on the structural features and the bonding situation of the quite unique title complex $[Pd(ZnCp^*)_4(ZnMe)_2\{Zn(tmeda)\}]$ (**1**).

Compound **1** dissolves in organic, nonpolar aromatic solvents such as benzene and toluene but is almost insoluble in *n*-hexane which allows facile separation from **2** and **3** and the Zn(II)

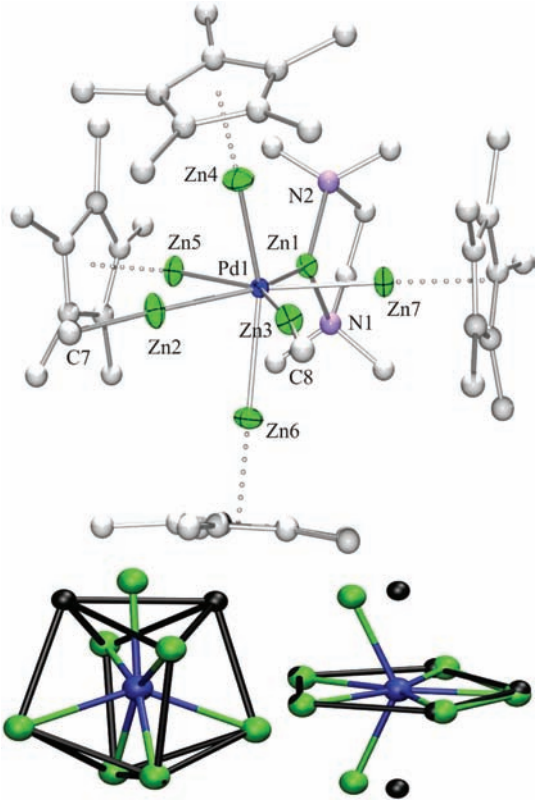

Figure 1. Above: Molecular structure of **1** in the solid state (PovRay plot; thermal ellipsoids for Pd and Zn are set at 50% probability; hydrogen atoms are omitted for clarity). Below: Superimpositions of the $[PdZn_7]$ metal cores (Pd, blue; Zn, green) with a trigonal dodecahedron (left) and a pentagonal bipyramid (right). Selected bond lengths [Å] and angles [deg]: Pd1−Zn1 2.389(1), Pd1−Zn2 2.385(1), Pd1−Zn3 2.396(1), Pd1−Zn4 2.454(1), Pd1−Zn5 2.476(1), Pd1−Zn6 2.453(1), Pd1−Zn7 2.480(1), Zn1−N1 2.140(4), Zn1−N2 2.125(4), Zn2−C7 1.972(5), Zn3−C8 1.981(6), Zn4-Cp*$_{centroid}$ 2.049, Zn5-Cp*$_{centroid}$ 2.061, Zn6-Cp*$_{centroid}$ 2.020, Zn7-Cp*$_{centroid}$ 2.030; Zn1−Zn5−Zn2 104.87(3), Zn7−Zn1−Zn5 115.04(3), Zn1−Pd1−Zn7 66.52(2), Zn3−Pd1−Zn7 75.83(2) Zn4−Pd1−Zn6 136.70(3), Pd1−Zn4−Cp*$_{centroid}$ 174.60, Pd1−Zn5−Cp*$_{centroid}$ 165.72, Pd1−Zn6−Cp*$_{centroid}$ 177.18, Pd1−Zn7−Cp*$_{centroid}$ 168.75.

byproduct mentioned above. In pure crystalline form **1** is stable for several weeks when stored under argon at −30 °C. The ^{1}H NMR spectrum (C_6D_6, room temperature.) shows resonances at 2.10 (s, br, 30H) and 2.26 (s, br, 30H) ppm which are assigned to two different sets of two equivalent ZnCp* units. Another signal at 0.14 (s, 6H) ppm is assigned to two chemically equivalent $ZnCH_3$ ligands. The presence of one tmeda ligand is indicated by the resonances at 1.62 (s, 4H) and 1.73 (s, 12H) ppm. The broadening of all the ZnCp* resonances suggests an exchange of the axial and equatorial Zn positions, i.e., Zn(4,6) and Zn(5,7) (for assignment see Figure 1). Both signals show coalescence at 50 °C giving rise to one broad signal at 2.18 (s, br, 60H) ppm. Further warm up to 70 °C gives rise to line sharpening (2.17 ppm; s, 60H) without significant changing in position and line width of the other resonances. The ^{13}C NMR spectrum shows no unusual features with respect to the expected signal pattern and can be looked up in the Experimental Section. LIFDI-MS of pure **1** nicely displays the molecular ion peak $[M]^{\bullet+}$ at m/z = 1252. The FT-IR spectrum shows characteristic absorption bands for

dx.doi.org/10.1021/ic201701r |*Inorg. Chem.* 2011, 50, 10486–10492

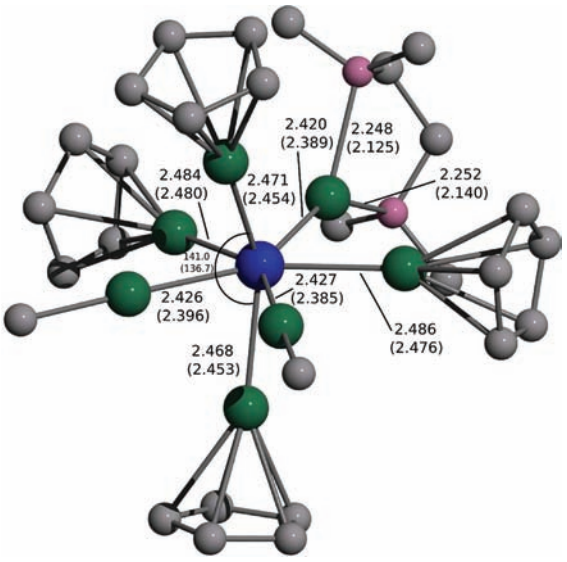

Figure 2. Calculated geometry of **1M**. Bond lengths are in Ångstroms, angles in degrees. Experimental values for **1** are given in parentheses.

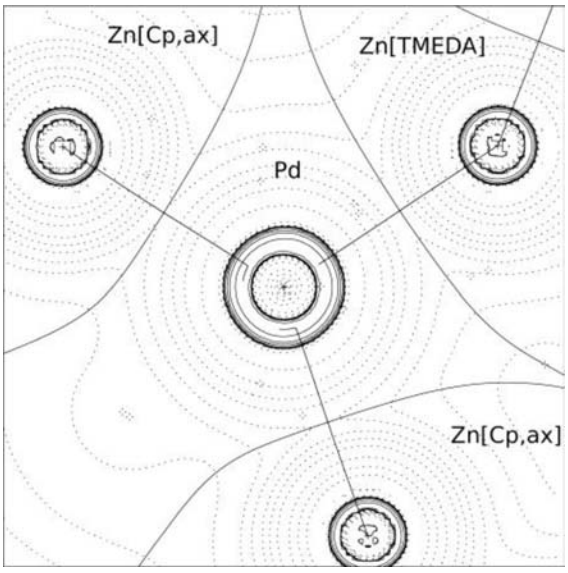

Figure 3. Molecular graph and contour map of the Laplacian $\nabla^2\rho(r)$ of **1M** in the molecular plane which contains Pd and the ligand atoms Zn($C_{p,ax}$) and Zn(TMEDA). Solid lines indicate areas of charge concentration ($\nabla^2\rho(r) < 0$), while dashed lines show areas of charge depletion ($\nabla^2\rho(r) > 0$). The thick solid lines connecting the atomic nulei are the bond paths. The thick solid lines separating the atomic basins indicate the zero-flux surfaces crossing the molecular plane.

the Cp* units as well as N−CH_3 and N−CH_2 absorptions in the typical range between 2950 and 2700 cm^{-1} (2931, 2867, 2829 cm^{-1} and broad absorptions at 2820−2780 cm^{-1}), which are quite well comparable with the respective features of GaCp* as well as ZnCp* containing reference complexes.

The molecular structure of **1** as determined by single crystal X-ray diffraction is depicted in Figure 1.

The Pd center is surrounded by three different types of Zn ligands, i.e., four ZnCp*, two ZnMe, and one {Zn(tmeda)} unit, resulting in an overall [$PdZn_7$] metal core. Such a mononuclear [PdE_7] core (E = any ligator atom) is unknown so far to the best of our knowledge. At first glance it may look obvious to describe the [$PdZn_7$] coordination environment in terms of a pentagonal bipyramid. The angles between the five "equatorial'" zinc ligator atoms Zn(1,2,3) and Zn(5,7) are ranging from 104.87(3)° (Zn2−Zn5−Zn1) to 115.04(3)° (Zn5−Zn1−Zn7) and yield an angle sum of 539.65°, which is quite close to the ideal value of 540°. However, a rigorous quantitative comparison of coordination polyhedra based on the continuous shape measure clearly shows a major distortion from a pentagonal bipyramid with a large value of $S_Q(P)$ = 4.30 (Figure 1; below, right).[24−26] The two ZnCp* ligands, i.e., Zn(4,6), are strongly bent toward both $ZnCH_3$ ligands, Zn(2,3). Nevertheless, the five ZnR ligands are almost coplanar as the corresponding shape measure of $S_Q(P)$ = 0.32 is small. An alternative description of the [$PdZn_7$] metal core structure is based on a deviation from an ideal trigonal dodecahedron (according to a [ML_8] type structure) with two corners being removed and substituted by one corner in between. This reasoning is nicely supported by the very small shape measure of $S_Q(P)$ = 0.07 when comparing the [$PdZn_7$] core of **1** with the corresponding six corners of an ideal trigonal dodecahedron (Figure 1; below, left).[27,28] Essentially, the {Zn(tmeda)} moiety (Zn1) rests almost exactly between the "missing" two corners of the dodecahedron. The related [$PdZn_8$] molecule, the octa-coordinated [$Pd(ZnCp^*)_4(ZnMe)_4$] features exactly such a dodecahedral structure.[15] Notably, these comparisons rule out further possible descriptions of the [$PdZn_7$] core as capped trigonal prismatic or capped octahedral environments. The perpendicular orientation of the tmeda substituent at Zn1 with respect to the planar Zn_5-ring minimizes the steric strain. For similar reasons the "axial" ZnCp* groups, Zn(4,6), are bent toward the "equatorial" $ZnCH_3$ with an angle of 136.70(3)° (Zn4−Pd1−Zn6). The ZnCp* units feature η^5-Cp* coordination with only small deviations of the Pd1−Zn−$Cp^*_{centroid}$ angles from the expected linearity (axial: Zn4, 174.60°; Zn6, 177.18°; equatorial: Zn5, 165.72°; Zn7, 168.75°). In addition, the Zn−$Cp^*_{centroid}$ distances ($Ø_{eq}$ = 2.045 Å and $Ø_{ax}$ = 2.035 Å) match very well with the reported distances of [$Zn_2Cp^*_2$] (Ø = 2.04 Å).[2] The Zn−N bond lengths at the terminal and tri-coordinated Zn1 (Ø = 2.133 Å) are quite matching with related tetra-coordinated terminal or bridging {Zn(tmeda)} moieties of some known transition metal complexes, such as $[(CO)_4Fe\{ZnCl(tmeda)\}_2]]$[29] (Ø = 2.174 Å) or $[\{(CO)_3Mn\}_2\{\mu$-$Zn(tmeda)\}(\mu$-$H)_2(\mu$-tedip)][30] (2.13(2) Å) (tedip = $(EtO)_2$-$POP(OEt)_2$). Interestingly and to the best of our knowledge, **1** is the first example for an unsupported terminally coordinated ZnL unit, in general. The Pd−Zn bond distances vary only by about 2% with an average value of 2.433 Å but nevertheless follow a trend, namely, Pd-$ZnCp^*_{eq}$ > Pd-$ZnCp^*_{ax}$ > Pd-ZnMe ≈ Pd−Zn(tmeda). The related Pd−Zn distances found for $[Pd(ZnCp^*)_4(ZnMe)_4]$[15] and $[Pd(ZnCp^*)_4(ZnZnCp^*)_4]$[16] are quite similar and range between 2.433(2) and 2.459(2) Å.

Table 1. Calculated NBO Partial Charges *q* for Atoms and Ligands in 1M

atom/ligand	*q* (NBO)
Pd	−3.05
Zn[tmeda]/(Zn{tmeda})	+0.79 (+1.11)
Zn[$C_{p,ax}$]/(ZnCp)	+0.92 (+0.33)/+0.89 (+0.30)
Zn[$C_{p,eq}$]/(ZnCp)	+0.81 (+0.25)/+0.81 (+0.25)
Zn[Me]/(ZnMe)	+0.95 (+0.40)/+0.95 (+0.41)

dx.doi.org/10.1021/ic201701r |*Inorg. Chem.* 2011, 50, 10486–10492

Table 2. EDA Results for the Pd-ZnR Interactions in 1M (Energies in kcal/mol, Distances in Å)

fragments	[Pd]/ZnMe	[Pd]/ZnC$_p$(ax)	[Pd]/ZnC$_p$(eq)	[Pd]/Zn(tmeda)
r(A−B)	2.427	2.471	2.486	2.420
ΔE_{int}	−74.5	−65.3	−70.8	−88.0
ΔE_{Pauli}	182.2	122.7	133.1	231.8
ΔE_{elstat}	−159.7 (62.2%)	−122.0 (64.9%)	−131.4 (64.4%)	−211.3 (66.1%)
ΔE_{orb}	−97.0 (37.8%)	−65.9 (35.1%)	−72.5 (35.6%)	−108.5 (33.9%)

These values are somewhat shorter as compared with the average Pd−Zn distance of 2.646 Å obtained for the Pd_1Zn_1 intermetallic phase, for example.[31] The Zn−Zn distances of **1** range between 2.6718(1) Å for Zn1−Zn7 and 2.997(1) Å for Zn3−Zn7 match very well with Zn−Zn contacts in the intermetallic phase Pd_1Zn_1 (2.899 Å).[31]

Analysis of the Bonding Situation by Density Functional Theory (DFT) Calculations. DFT calculations of the model compound **1M** where the Cp* ligands are replaced by Cp have been carried out at the BP86/TZVPP level (for details see Experimental Section and Supporting Information) to elucidate the nature of the metal−ligand bonding situation and in particular to compare the electronic situation of the three different types of Zn ligands. The optimized geometry of **1M** and the most important bond lengths are given in Figure 2. The calculated Pd−Zn distances in **1M** are slightly longer than the experimental values for **1**, but the differences are not very large. Both sets of data give the same trend for the distances Pd-ZnCp(*)$_{eq}$ > Pd-ZnCp(*)$_{ax}$ > Pd-ZnMe ≈ Pd−Zn(tmeda). The calculated bond angle between the axial ligands Zn4−Pd1−Zn6 (141.0°) in **1M** also concurs with the experimental value (136.7°) in **1**. Thus, we may use **1M** as a model for the analysis of the bonding situation in **1**.

Our previous studies of transition metal complexes [M(ZnR)$_n$] that carry one-electron donor ligands ZnR (R = Me, Cp) have shown that there are strong M-ZnR bonds, while the Zn−Zn interactions between the ligands are only weakly attractive.[14−16,32] The atoms in molecules (AIM) analysis of the electronic structure of [M(ZnR)$_n$] complexes showed that there are always M-ZnR bond paths, while most compounds do not exhibit Zn−Zn bond paths. Figure 3 shows the Laplacian distribution of **1M** in the plane which contains Pd and the ligand atoms Zn(Cp,ax) and Zn(tmeda). There are three Pd−Zn bond paths but there are no Zn−Zn bond paths. The same result is obtained for the other Zn ligands in **1M**.

The shape of the Laplacian distribution in **1M** does not exhibit a difference between ZnCp and {Zn(tmeda)}. Significant differences are found, however, between the calculated NBO partial charges of the different ligands. The Pd atom in **1M** carries a large negative charge of −3.05e, while the Zn atoms of the ligands are positively charged (Table 1). Interestingly, the Zn atom of {Zn(tmeda)} has a positive charge (+0.79e), which is very close to the other Zn atoms (between +0.81 and +0.95e) and is not very different from the charge of +0.72e calculated for the Zn atoms in [$Zn_2Cp^*_2$]. However, the charge of the {Zn(tmeda)} ligand as a whole is much higher (+1.11e) than for the other Zn-ligands (between +0.25 and +0.41e). The energy decomposition analysis (EDA) revealed also significant differences between the Pd-ZnR and Pd−Zn(tmeda) interactions in **1M** (Table 2). The overall strength of the Pd−Zn interactions ΔE_{int} for the latter ligand is somewhat larger than for the former, while the relative contributions of the attractive terms ΔE_{elstat} and ΔE_{orb} to the total interactions energy are very similar for the two types of ligands. However, the Pauli repulsion ΔE_{Pauli} for the Pd−Zn-(tmeda) bond is much higher than for Pd-ZnMe and Pd-ZnCp. This is compensated by the nearly equally strong increase in the ΔE_{elstat} and ΔE_{orb} values for Pd−Zn(tmeda). The results show that it can be useful to inspect the absolute values of the EDA energy terms for gaining insight into the variation between different metal−ligand interactions.

The structural data of **1** and the overall features of the bonding situation of **1M** indicates that **1** is nothing else but a seven-coordinated variant of [Pd(ZnCp*)$_4$(ZnMe)$_4$] where two $ZnCH_3$ ligands are replaced by one {Zn(tmeda)} ligand. The whole family of compounds [M(ZnR)$_n$] and [M(ZnR)$_a$(GaR)$_b$] ($a + 2b = n \geq 8$) fulfills the 18 valence electron rule with ZnR regarded as one electron and GaR regarded as two electron donor ligands and assigning the formal oxidation state M(0) to the central transition metal. Also note, the structures of the Zn/Ga mixed compounds can be derived from the homoleptic parent compounds [M(ZnR)$_n$] in the same way as we discussed the relation of [Pd(ZnCp*)$_4$(ZnMe)$_4$] and **1** above.[14−16,32] Obviously, the {Zn(tmeda)} ligand is electronically equivalent to two ZnR ligands and quite similar to one GaR ligand. This reasoning suggests a treatment of the {Zn(tmeda)} ligand as a strong two electron donor ligand with the formal oxidation state Zn(0). This assignment is in qualitative agreement with the calculated NBO partial charge of Pd in **1M** (−3.05e), which is significantly higher than in [Pd(ZnH)$_8$] (−1.95e).[33] The bigger donor strength of {Zn(tmeda)} compared with Zn(Cp) and $ZnCH_3$ comes also to the fore by the calculated partial charges of the ligands in **1M** (Table 1). Clearly, the analysis of the electronic structure reveals significant differences between the one electron and two electron donors as it is expected if Zn atoms in Zn(Cp) and $ZnCH_3$ are viewed as Zn(I) species while Zn(0) is assigned for {Zn(tmeda)}. We want to point out, however, that there is generally no correlation between the partial charges and the oxidation state of an atom.

The isolation of **1** let it seems feasible that more than one terminal unit ZnL_n can substitute M′R ligands (M′ = Zn, Cd, Al, Ga, In; R = Me, Cp*) in the compounds [M(M′R)$_n$], which could lead to species such as [Pd(ZnCp*)$_4${Zn(tmeda)}$_2$] or even [Pd{Zn(tmeda)}$_4$]. It seems, however, that further substitution of two ligands Zn(Cp*) or $ZnCH_3$ by {Zn(tmeda)} is energetically unfavorable because hypothetical 18 electron species such as [Pd(ZnCp*)$_4${Zn(tmeda)}$_2$] or [Pd{Zn(tmeda)}$_4$] are not even observed as trace products, so far. We will carry out theoretical studies of the relative bond strength of the two electron donor {Zn(tmeda)} and two one electron donors ZnR in future work.

CONCLUSIONS

The synthesis of [Pd(ZnCp*)$_4$(ZnMe)$_2${Zn(tmeda)}] (**1**) nicely points out the particularly rich chemistry of Carmonas

reagent $[Zn_2Cp^*_2]$ in combination with substitution labile transition metal complexes. It serves as transfer reagent for Cp*, ZnCp*, {ZnZnCp*}, and even Zn(0) depending on substituents R and ligands L at the transition metal side. The formation of **1** involves several competing or rather interconnected reaction pathways such as homolytic bond cleavage, Cp^*/CH_3 exchange sequences, and redox chemical processes. The main structural feature of **1** is the unprecedented $[PdZn_7]$ metal core that can be most likely deviated from known $[ML_8]$ structures found in the zinc-rich compounds $[M(ZnCp^*)_4(ZnMe)_4]$ (M = Ni, Pd, Pt). This finding has been quantitatively described by a very low continuous shape measure. Additionally, quantum chemical calculations by means of AIM and EDA analysis show significant differences in the metal-to-ligand bonding situations of the different kinds of ZnR at which the organic group R plays an important role. The products seem to be thermodynamically controlled with the 18 valence electron rule as a reliable heuristic guide for rationalization of products and for synthesis planning. In the presence of stoichiometric amounts of Lewis base ligands L, as it is the case for $[Pd(CH_3)_2(tmeda)]$ as the reaction partner, zinc-rich compounds with various types of Zn-ligands such as **1** can be obtained in good yields. The concept may be applicable to other reactive transition metal starting compounds of the general type $[L_nMR_m]$ and investigations to identify suitable candidates and reaction conditions are underway.

EXPERIMENTAL SECTION

General Techniques and Analytical Methods. All manipulations were carried out in an atmosphere of purified argon using standard Schlenk and glovebox techniques. *n*-Hexane and toluene were dried using an mBraun Solvent Purification System. The final H_2O content in all solvents used was checked by Karl Fischer-Titration and did not exceed 5 ppm. $[Pd(CH_3)_2(tmeda)]$[34] and $[Zn_2Cp^*_2]$[1] were prepared according to literature methods. Elemental analyses were performed by the Microanalytical Laboratory of the University of Bochum. NMR spectra were recorded on a Bruker Avance DPX-250 spectrometer (^1H, 250.1 MHz; ^{13}C, 62.9 MHz) in C_6D_6 and CD_2Cl_2 at 298 K unless otherwise stated. Chemical shifts are given relative to TMS and were referenced to the solvent resonances as internal standards. FT-IR spectra were measured in an ATR setup with a Bruker Alpha FTIR spectrometer under inert atmosphere in a glovebox. Mass spectrometry was measured with a Jeol AccuTOF GCv. Ionization method: FD (LIFDI). Solvent: toluene.

Synthesis. *[Pd(ZnCp*)$_4$(ZnMe)$_2${Zn(tmeda)}] (**1**).* $[Pd(CH_3)_2(tmeda)]$ (0.060 g, 0.237 mmol) and $[Zn_2Cp^*_2]$ (0.390 mg, 0.974 mmol) were dissolved in toluene (6 mL), resulting in a deep red clear solution. The mixture was stirred for 1 h at 55 °C, the solvent reduced in vacuo, the yellow-orange residue washed with *n*-hexane (3 × 3 mL) and dried in vacuo to give a yellow solid. Recrystallization of the crude product in a mixture of toluene/*n*-hexane (3 mL/2 mL) at −30 °C overnight gave yellow single crystals that contain one molecule toluene and *n*-hexane per formula unit of **1** (see Table 3). Yield: 0.105 g (35%). Analytical and spectroscopic data were obtained after removing crystal solvent molecules in vacuo. Anal. Calcd. for $C_{48}H_{82}N_2Zn_7Pd_1$: C, 46.07; H, 6.61. Found: C, 46.22; H, 6.96. ^1H NMR $\delta_H(C_6D_6)$, 0.14 (s, 6H, ZnMe), 1.62 (s, 4H, $(CH_3)_2N-CH_2-CH_2-N(CH_3)_2$), 1.73 (s, 12H, $(CH_3)_2N-CH_2-CH_2-N(CH_3)_2$), 2.10 (s, br, 30H, C_5Me_5), 2.27 (s, br, 30H, C_5Me_5). ^1H NMR $\delta_H(C_6D_6$, 50 °C), 0.10 (s, 6H, ZnMe), 1.71 (s, 4H, $(CH_3)_2N-CH_2-CH_2-N(CH_3)_2$), 1.79 (s, 12H, $(CH_3)_2N-CH_2-CH_2-N(CH_3)_2$), 2.17 (s, br, 60H, C_5Me_5). ^1H NMR $\delta_H(C_6D_6$, 70 °C), 0.07 (s, 6H, ZnMe), 1.76 (s, 4H, $(CH_3)_2N-CH_2-CH_2-N(CH_3)_2$), 1.83 (s, 12H, $(CH_3)_2N-CH_2-CH_2-N(CH_3)_2$), 2.17 (s, 60H, C_5Me_5). ^1H NMR $\delta_H(CD_2Cl_2)$, −0.41 (s, 6H, ZnMe), 2.01 (s, br, 60H, C_5Me_5), 2.28 (s, 12H, $(CH_3)_2N-CH_2-CH_2-N(CH_3)_2$), 2.67 (s, 4H, $(CH_3)_2N-CH_2-CH_2-N(CH_3)_2$). $^{13}C\{^1H\}$ NMR $\delta_{C\{H\}}(C_6D_6)$, 111.10 (ZnC_5Me_5), 109.91 (ZnC_5Me_5), 55.08 ($(CH_3)_2N-CH_2-CH_2-N(CH_3)_2$), 46.23 ($(CH_3)_2N-CH_2-CH_2-N(CH_3)_2$)), 14.22 (ZnMe), 12.18 (ZnC_5Me_5), 11.91 (ZnC_5Me_5). IR (ATR, cm^{-1}): 2867 (s), 2829 (s), 2698 (w), 1447 (m), 1427 (w), 1408 (w), 1363 (m), 1277 (w), 1250 (w), 1178 (w), 1152 (w), 1130 (w), 1115 (w), 1088 (w), 1038 (w), 1019 (w), 1001 (m), 941 (w), 786 (s), 757 (w), 722 (m), 688 (w), 633 (w), 583 (w), 523 (s), 476 (w), 460 (w), 429 (w), 403 (w). MS (LIFDI, toluene): *m*/*z* 1252 $[M]^{\cdot+}$.

Table 3. Crystallographic Data and Refinement Details for $1\cdot C_7H_5\cdot C_6H_{14}$

empirical formula	$C_{58}H_{97}N_2PdZn_7$	$\rho_{calc.}$ (g cm^{-3})	1.489
M_r	1386.37	μ (mm^{-1})	2.984
T (K)	113(2)	F (000)	2860
λ (Å)	0.71073	$2\theta_{max}$ (deg)	53
crystal size (mm^3)	0.30 × 0.25 × 0.20	reflections collected	76686
crystal system	monoclinic	reflections unique	12817
space group	$P2_1/n$	R_{int}	0.1399
a (Å)	12.3193(4)	reflections observed [$I > 2\sigma(I)$]	8134
b (Å)	23.4719(9)	parameters/restraints	623/50
c (Å)	21.3947(8)	goodness-of-fit on F^2	1.016
β (°)	90.851(4)	R_1 [$I > 2\sigma(I)$]	0.0545
V (Å^3)	6185.8(4)	wR_2 (all data)	0.1027
Z	4	residuals (e Å^{-3})	0.578/−0.656

Single-Crystal X-ray Diffraction. The single-crystal X-ray diffraction intensities of $1\cdot C_7H_5\cdot C_6H_{14}$ ($C_{58}H_{97}N_2PdZn_7$) were collected on an Oxford Xcalibur^{TM}2 diffractometer with a Sapphire2 CCD. The crystal structure was solved by direct methods using SHELXS-97 and refined with SHELXL-97.[35] The crystals were coated with a perfluoropolyether, picked up with a glass fiber, and immediately mounted in the cooled nitrogen stream of the diffractometer. Selected crystallographic data collection and structure solution parameters are given in Table 3. CCDC 830670 (**1**) contains the full set of crystallographic data for this paper. These data can be obtained free of charge from The Cambridge Crystallographic Data Centre via www.ccdc.cam.ac.uk/data_request/cif.

Computational Methods. The structural parameters of the model compound **1M** where Cp* is replaced by Cp were optimized at BP86/def2-TZVPP[36−38] with the Gaussian 03, revision E.01,[39] algorithm using energies calculated with the Turbomole 6.3[40] program package. The RI approximation[41] was applied using auxiliary basis functions.[42] EDA were carried out at BP86/TZ2P using the ADF(2009.01) program package.[43] Uncontracted Slater-type orbitals (STOs) were employed as basis functions in self-consistent field (SCF) calculations.[44] Triple-ζ-quality basis sets were used which were augmented by two sets of polarization functions, that is, p and d functions for the hydrogen atom and d and f functions for the other atoms. An auxiliary set of s, p, d, f, and g STOs was used to fit the molecular densities and to represent the Coulomb and exchange potentials accurately in each SCF cycle.[45] Scalar relativistic effects were considered using the zero-order regular approximation (ZORA).[46] Within the EDA, bond formation between the interacting fragments is divided into three steps: In the first step, the fragments, which are calculated with the frozen geometry that they possess in the entire molecule, are superimposed without electronic relaxation to yield the quasiclassical electrostatic attraction ΔE_{elstat}. In the second step, the

product wave function becomes antisymmetrized and renormalized, which gives the Pauli repulsion ΔE_{Pauli}. The third step consists of the relaxation of the molecular orbitals to their final form to yield the stabilizing orbital interactions ΔE_{orb}. The sum of the three terms ΔE_{elstat} + ΔE_{Pauli} + ΔE_{orb} gives the total interaction energy ΔE_{int}. The NBO[47] charges were obtained using the NBO 3.1 program implemented in Gaussian03. The AIM[48] analyses were carried out using a modified version of AIMPAC[49] using a BP86/def2-SVP wave function.

■ ASSOCIATED CONTENT

Supporting Information. IR and LIFDI-MS spectra of **1** and Cartesian coordinates of the calculated model compound **1M**. This material is available free of charge via the Internet at http://pubs.acs.org.

■ AUTHOR INFORMATION

Corresponding Author
*E-mail: roland.fischer@ruhr-uni-bochum.de. Fax (+49)234 321 4174.

■ ACKNOWLEDGMENT

This work has been funded by the German Research Foundation (DFG, Fi 502/23-1 und Fr 641/23-1). T.B. and M.M. are grateful for PhD scholarships by the Fonds der Chemischen Industrie, Germany, and for support by the Ruhr University Research School (http://www.research-school.rub.de/). The authors would like to thank the Linden CMS GmbH, Germany, and S. Bendix (Ruhr University Bochum) for support in mass spectrometry.

■ REFERENCES

(1) Resa, I.; Carmona, E.; Gutierrez-Puebla, E.; Monge, A. *Science* **2004**, *305*, 1136. del Rio, D.; Galindo, A.; Resa, I.; Carmona, E. *Angew. Chem., Int. Ed.* **2005**, *44*, 1244.

(2) (a) Grirrane, A.; Resa, I.; Rodriguez, A.; Carmona, E.; Alvarez, E.; Gutierrez-Puebla, E.; Monge, A.; Galindo, A.; Del Rio, D.; Andersen, R. A. *J. Am. Chem. Soc.* **2007**, *129*, 693. (b) del Rio, D.; Galindo, A.; Resa, I.; Carmona, E. *Angew. Chem., Int. Ed.* **2005**, *44*, 1244.

(3) (a) Zhu, Z.; Brynda, M.; Wright, R. J.; Fischer, R. C.; Merrill, W. A.; Rivard, E.; Wolf, R.; Fettinger, J. C.; Olmstead, M. M.; Power, P. P. *J. Am. Chem. Soc.* **2007**, *129*, 10847. (b) Nayek, H. P.; Luehl, A.; Schulz, S.; Koeppe, R.; Roesky, P. W. *Chem.—Eur. J.* **2011**, *17*, 1773. (c) Schulz, S.; Gondzik, S.; Schuchmann, D.; Westphal, U.; Dobrzycki, L.; Boese, R.; Harder, S. *Chem. Commun.* **2010**, *46*, 7757. (d) Zhu, Z.; Wright, R. J.; Olmstead, M. M.; Rivard, E.; Brynda, M.; Power, P. P. *Angew. Chem., Int. Ed.* **2006**, *45*, 5807. (e) Liu, Y.; Li, S.; Yang, X.-J.; Yang, P.; Gao, J.; Xia, Y.; Wu, B. *Organometallics* **2009**, *28*, 5270. (f) Wang, Y.; Quillian, B.; Wei, P.; Wang, H.; Yang, X.-J.; Xie, Y.; King, R. B.; Schleyer, P. V. R.; Schaefer, H. F., III; Robinson, G. H. *J. Am. Chem. Soc.* **2005**, *127*, 11944. (g) Fedushkin, I. L.; Skatova, A. A.; Ketkov, S. Y.; Eremenko, O. V.; Piskunov, A. V.; Fukin, G. K. *Angew. Chem., Int. Ed.* **2007**, *46*, 4302. (h) Yang, X.-J.; Yu, J.; Liu, Y.; Xie, Y.; Schaefer, H. F.; Liang, Y.; Wu, B. *Chem. Commun.* **2007**, *23*, 2363. (i) Tsai, Y.-C.; Lu, D.-Y.; Lin, Y.-M.; Hwang, J.-K.; Yu, J.-S. K. *Chem. Commun.* **2007**, *40*, 4125. (j) Yu, J.; Yang, X.-J.; Liu, Y.; Pu, Z.; Li, Q.-S.; Xie, Y.; Schaefer, H. F.; Wu, B. *Organometallics* **2008**, *27*, 5800.

(4) Kress, J. W. *J. Phys. Chem.* **2005**, *109*, 7757.

(5) del Rio, D.; Resa, I.; Rodriguez, A.; Sanchez, L.; Koppe, R.; Downs, A. J.; Tang, C. Y.; Carmona, E. *J. Phys. Chem.* **2008**, *112*, 10516.

(6) Philpott, M. R.; Kawazoe, Y. *Chem. Phys.* **2006**, *327*, 283.

(7) Hepperle, S. S.; Wang, Y. A. *J. Phys. Chem.* **2008**, *112*, 9619.

(8) Schulz, S.; Schuchmann, D.; Westphal, U.; Bolte, M. *Organometallics* **2009**, *28*, 1590.

(9) Schulz, S.; Schuchmann, D.; Krossing, I.; Himmel, D.; Blaeser, D.; Boese, R. *Angew. Chem., Int. Ed.* **2009**, *48*, 5748.

(10) Schuchmann, D.; Westphal, U.; Schulz, S.; Florke, U.; Blaser, D.; Boese, R. *Angew. Chem., Int. Ed.* **2009**, *48*, 807.

(11) Gondzik, S.; Blaeser, D.; Woelper, C.; Schulz, S. *Chem.—Eur. J.* **2010**, *16*, 13599.

(12) Carrasco, M.; Peloso, R.; Rodriguez, A.; Alvarez, E.; Maya, C.; Carmona, E. *Chem.—Eur. J.* **2010**, *16*, 9754.

(13) Carrasco, M.; Peloso, R.; Resa, I.; Rodriguez, A.; Sanchez, L.; Alvarez, E.; Maya, C.; Andreu, R.; Calvente, J. J.; Galindo, A.; Carmona, E. *Inorg. Chem.* **2011**, *50*, 6361.

(14) Cadenbach, T.; Bollermann, T.; Gemel, C.; Fernandez, I.; von Hopffgarten, M.; Frenking, G.; Fischer, R. A. *Angew. Chem., Int. Ed.* **2008**, *47*, 9150.

(15) Cadenbach, T.; Bollermann, T.; Gemel, C.; Tombul, M.; Fernandez, I.; von Hopffgarten, M.; Frenking, G.; Fischer, R. A. *J. Am. Chem. Soc.* **2009**, *131*, 16063.

(16) Bollermann, T.; Freitag, K.; Gemel, C.; Seidel, R. W.; von Hopffgarten, M.; Frenking, G.; Fischer, R. A. *Angew. Chem., Int. Ed.* **2011**, *50*, 772.

(17) Bollermann, T.; Freitag, K.; Gemel, C.; Seidel, R. W.; Fischer, R. A. *Organometallics* **2011**, *30* (15), 4123.

(18) Steinke, T.; Gemel, C.; Winter, M.; Fischer, R. A. *Angew. Chem., Int. Ed.* **2002**, *41*, 4761.

(19) Budzelaar, P. H. M.; Boersma, J.; Van der Kerk, G. J. M.; Spek, A. L.; Duisenberg, A. J. M. *Organometallics* **1985**, *4*, 680.

(20) Fischer, B.; Boersma, J.; Van Koten, G.; Spek, A. L. *New J. Chem.* **1988**, *12*, 613.

(21) Fischer, B.; Kleijn, H.; Boersma, J.; Van Koten, G.; Spek, A. L. *Organometallics* **1989**, *8*, 920.

(22) Budzelaar, P. H. M.; Boersma, J.; Van der Kerk, G. J. M. *Angew. Chem.* **1983**, *95*, 335.

(23) Bollermann, T.; Molon, M.; Gemel, C.; Freitag, K.; Seidel, R. W.; von Hopffgarten, M.; Jerabek, P.; Frenking, G.; Fischer, R. A. 2011, submitted.

(24) Zabrodsky, H.; Peleg, S.; Avnir, D. *J. Am. Chem. Soc.* **1992**, *114*, 7843.

(25) Zabrodsky, H.; Peleg, S.; Avnir, D. *J. Am. Chem. Soc.* **1993**, *115*, 8278.

(26) Pinsky, M.; Avnir, D. *Inorg. Chem.* **1998**, *37*, 5575.

(27) Cirera, J.; Ruiz, E.; Alvarez, S. *Organometallics* **2005**, *24*, 1556.

(28) Drew, M. G. B. *Coord. Chem. Rev.* **1977**, *24*, 179.

(29) Fuhr, O.; Fenske, D. *Z. Anorg. Allg. Chem.* **2000**, *626*, 1822.

(30) Riera, V.; Ruiz, M. A.; Tiripicchio, A.; Tiripicchio-Camellini, M. *Organometallics* **1993**, *12*, 2962.

(31) Nowotny, H.; Bittner, H. *Monatsh. Chem.* **1950**, *81*, 679.

(32) Bollermann, T.; Cadenbach, T.; Gemel, C.; von Hopffgarten, M.; Frenking, G.; Fischer, R. A. *Chem.—Eur. J.* **2010**, *16*, 13372.

(33) In ref 15, we report a partial charge q(Pd) in $[Pd(ZnH)_8]$ of +0.09 e which was calculated with the Hirshfeld method. We lately found that the calculated values for the partial charges using the Hirshfeld method strongly depends on the reference state of the atoms, which makes it less useful particularly for transition metals.

(34) De Graaf, W.; Boersma, J.; Smeets, W. J. J.; Spek, A. L.; Van Koten, G. *Organometallics* **1989**, *8*, 2907.

(35) Sheldrick, G. M. *Acta Crystallogr.* **2008**, *A64*, 112.

(36) Becke, A. D. *Phys. Rev. A* **1988**, *38*, 3098.

(37) Perdew, J. *Phys. Rev. B* **1986**, *33*, 8822.

(38) F. Weigend, F.; R. Ahlrichs, R. *Phys. Chem. Chem. Phys.* **2005**, *7*, 3297.

(39) Frisch, M. J.; Trucks, G. W.; Schlegel, H. B.; Scuseria, G. E.; Robb, M. A.; Cheeseman, J. R.; Montgomery, J. A., Jr.; Vreven, T.; Kudin, K. N.; Burant, J. C.; Millam, J. M.; Iyengar, S. S.; Tomasi, J.; Barone, V.; Mennucci, B.; Cossi, M.; Scalmani, G.; Rega, N.; Petersson, G. A.; Nakatsuji, H.; Hada, M.; Ehara, M.; Toyota, K.; Fukuda, R.; Hasegawa, J.; Ishida, M.; Nakajima, T.; Honda, Y.; Kitao, O.; Nakai, H.;

Klene, M.; Li, X.; Knox, J. E.; Hratchian, H. P.; Cross, J. B.; Bakken, V.; Adamo, C.; Jaramillo, J.; Gomperts, R.; Stratmann, R. E.; Yazyev, O.; Austin, A. J.; Cammi, R.; Pomelli, C.; Ochterski, J. W.; Ayala, P. Y.; Morokuma, K.; Voth, G. A.; Salvador, P.; Dannenberg, J. J.; Zakrzewski, V. G.; Dapprich, S.; Daniels, A. D.; Strain, M. C.; Farkas, O.; Malick, D. K.; Rabuck, A. D.; Raghavachari, K.; Foresman, J. B.; Ortiz, J. V.; Cui, Q.; Baboul, A. G.; Clifford, S.; Cioslowski, J.; Stefanov, B. B.; Liu, G.; Liashenko, A.; Piskorz, P.; Komaromi, I.; Martin, R. L.; Fox, D. J.; Keith, T.; Al-Laham, M. A.; Peng, C. Y.; Nanayakkara, A.; Challacombe, M.; Gill, P. M. W.; Johnson, B.; Chen, W.; Wong, M. W.; Gonzalez, C.; Pople, J. A. *Gaussian 03*, revision E.01; Gaussian, Inc.: Wallingford, CT, 2004.

(40) Ahlrichs, R.; Bär, M.; Häser, M.; Horn, H.; Kölmel, C. *Chem. Phys. Lett.* **1989**, *162*, 165.

(41) Ahlrichs, R. *Phys. Chem. Chem. Phys.* **2004**, *6*, 5119.

(42) (a) Eichkorn, K.; Treutler, O.; Öhm, H.; Häser, H.; Ahlrichs, R. *Chem. Phys.* **1995**, *242*, 652. (b) Eichkorn, K.; Weigend, F.; Treutler., O.; Ahlrichs, R. *Theor. Chem. Acc.* **1997**, *97*, 119. (c) Weigend, F. *Phys. Chem. Chem. Phys.* **2006**, *8*, 1057.

(43) ADF2009.01, SCM, *Theoretical Chemistry*; Vrije Universiteit: Amsterdam, http://www.scm.com.

(44) Snijders, J. G.; Vernooijs, P.; Baerends, E. J. *Atom. Data Nucl. Data Tables* **1981**, *26*, 483.

(45) Krijn, J.; Baerends, E. J. *Internal Report: Fit Functions in the HFSMethod*; Vrije Universiteit: Amsterdam, 1984.

(46) (a) Chang, C.; Pelissier, M.; Durand, P. *Phys. Scr.* **1986**, *34*, 394. (b) Heully, J.-L.; Lindgren, I.; Lindroth, E.; Lundqvist, S.; Martensson-Pendrill, A.-M. *J. Phys. B* **1986**, *19*, 2799. (c) Snijders, J. *Chem. Phys. Lett.* **1996**, *252*, 51. (d) Lenthe, E. V.; Baerends, E. J.; Snijders, J. G. *J. Chem. Phys.* **1993**, *99*, 4597. (e) van Lenthe, E.; van Leeuwen, R.; Baerends, E. J.; Snijders, J. G. *Int. J. Quantum Chem.* **1996**, *57*, 281.

(47) (a) Reed, A. E.; Weinstock, R. B.; Weinhold, F. *J. Chem. Phys.* **1985**, *83*, 735. (b) Reed, A. E.; Curtiss, L. A.; Weinhold, F. *Chem. Rev.* **1988**, *88*, 899.

(48) Bader, R. F. W. *Atoms in Molecules: A Quantum Theory*; University of Oxford Press: Oxford, 1990.

(49) *AIMPAC*: http://www.chemistry.mcmaster.ca/aimpac.